INTERNATIONAL JOURNAL FOR NUMERICAL METHODS IN FLUIDS, VOL. 8, 705–722 (1988)

MAGNETOHYDRODYNAMIC FLOW IN ELECTRODYNAMICALLY COUPLED RECTANGULAR DUCTS

MUNEVVER SEZGIN

Department of Mathematics, Middle East Technical University, Ankara, Turkey

SUMMARY

In Sezgin[1,2] the problems considered are the magnetohydrodynamic (MHD) flows in an electrodynamically conducting infinite channel and in a rectangular duct respectively, in the presence of an applied magnetic field. In the present paper we extend the solution procedure of these papers to two rectangular channels connected by a barrier which is partially conductor and partially insulator. The problem has been reduced to the solution of a pair of dual series equations and then to the solution of a Fredholm's integral equation of the second kind. The infinite series obtained were transformed to finite integrals containing Bessel functions of the second kind to avoid the computations of slowly converging infinite series and infinite integrals with oscillating integrands. The results obtained compared well with those of Butsenieks and Shcherbinin[3] which were obtained for the perfectly conducting barrier separating the flows.

KEY WORDS MHD flow Connected channels Ducts

INTRODUCTION

We consider the steady laminar flow of an incompressible, viscous, electrically conducting fluid in connected rectangular ducts where the geometry is as shown in Figure 1. The axis of the ducts is chosen as the z-axis. A uniform magnetic field of strength H_0 is directed along the axis of x. The walls parallel to the magnetic field are insulated and the walls perpendicular to the magnetic field at $x=a_1$ and $x=-a_2$ are also insulated, but the wall (barrier) perpendicular to the magnetic field at $x=0$ is partly conductor and partly insulator (conducting for a length l from the origin symmetrically). The first flow I is separated from the second flow II by this thin partition.

In this arrangement the fluid in channel I is driven by a pressure gradient Δp_1, which is produced by a pump, and the transfer of hydraulic energy to channel II, which is connected to some hydraulic load, is done electrodynamically, since part of the current induced by flow I, through the conducting partition, forms a closed current loop which passes into channel II and which, by interacting with the transverse magnetic field, generates a force in the direction of the positive z-axis (in the direction of flow I). Also the flow II is subject to a pressure gradient Δp_2 which depends on the hydraulic load of channel II.

The system of equations for uniform flows in channels I and II, namely the z-components of the momentum equation and the curl of Ohm's law (for identical fluids of density ρ, coefficient of viscosity μ, magnetic permeability μ_e and electrical conductivity σ), can be written as[4]

$$\mu\nabla^2 V_1 + \mu_e H_0 \partial H_1/\partial x = \partial P_1/\partial z, \tag{1}$$

0271–2091/88/060705–18$09.00

Received 19 January 1987
Revised 13 August 1987

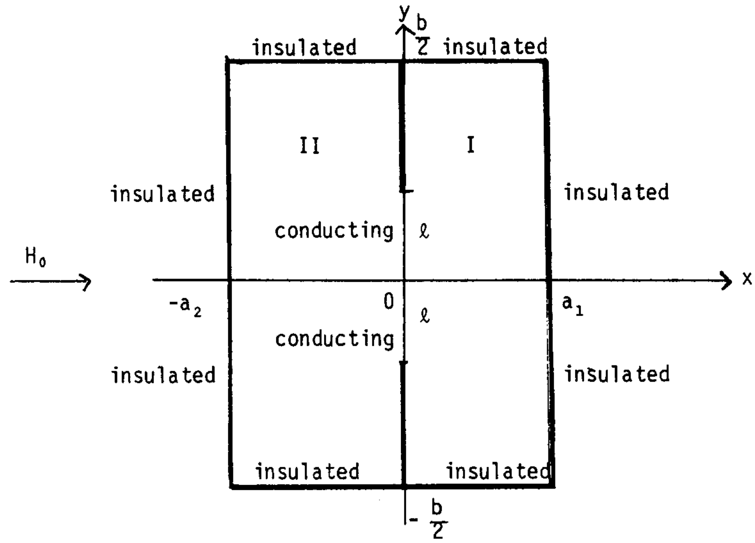

Figure 1. The geometry of the problem

$$\eta\nabla^2 H_1 + H_0 \partial V_1/\partial x = 0, \tag{2}$$

$$\mu\nabla^2 V_2 + \mu_e H_0 \partial H_2/\partial x = \partial P_2/\partial z, \tag{3}$$

$$\eta\nabla^2 H_2 + H_0 \partial V_2/\partial x = 0, \tag{4}$$

where the subscripts 1 and 2 refer to the dimensional quantities in the direction of the z-axis in channels I and II respectively and $\eta = (\sigma\mu_e)^{-1}$. The non-dimensionalization is performed with a characteristic length (the width of the right channel a_1) and reference values for the velocities in both channels ($V_{0_{1,2}} = -a_1^2(\partial P_{1,2}/\partial z)/\mu$). So the equations for the velocities $V_1(x, y)$, $V_2(x, y)$ and the induced magnetic fields $B_1(x, y)$, $B_2(x, y)$ for channels I and II respectively are (using the notations V, B for V_1, B_1 and $\bar{V}$, $\bar{B}$ for V_2, B_2 after non-dimensionalization)

$$\nabla^2 V + M\partial B/\partial x = -1, \tag{5}$$

$$\nabla^2 B + M\partial V/\partial x = 0, \tag{6}$$

$$\nabla^2 \bar{V} + M\partial \bar{B}/\partial x = k, \tag{7}$$

$$\nabla^2 \bar{B} + M\partial \bar{V}/\partial x = 0, \tag{8}$$

where

$$k = -\frac{\partial P_2}{\partial z}\bigg/\frac{\partial P_1}{\partial z} \tag{9}$$

and M is the Hartmann number. The parameter k is actually positive, since the pressure gradient produced in channel II is in the direction of the fluid motion, while in channel I the direction of the pressure gradient is opposite to the flow direction.

The boundary conditions for systems (5)–(8) are the following. The velocity everywhere at the solid walls is zero; the induced magnetic field is zero everywhere at the non-conducting walls and continuous on the conducting partition separating the flows:

$$V(0, y) = V(1, y) = 0; \quad -b/2 \leqslant y \leqslant b/2, \tag{10a}$$

$$V(x, -b/2) = V(x, b/2) = 0; \quad 0 \leqslant x \leqslant 1, \tag{10b}$$

$$\bar{V}(0, y) = \bar{V}(-\alpha_2, y) = 0; \quad -b/2 \leqslant y \leqslant b/2, \; \alpha_2 = a_2/a_1, \tag{10c}$$

$$\bar{V}(x, b/2) = \bar{V}(x, -b/2) = 0; \quad -\alpha_2 \leqslant x \leqslant 0, \; b = b/a_1, \tag{10d}$$

$$B(1, y) = 0; \quad -b/2 \leqslant y \leqslant b/2, \tag{10e}$$

$$\bar{B}(-\alpha_2, y) = 0; \quad -b/2 \leqslant y \leqslant b/2, \tag{10f}$$

$$B(x, -b/2) = B(x, b/2) = 0; \quad 0 \leqslant x \leqslant 1, \tag{10g}$$

$$\bar{B}(x, -b/2) = \bar{B}(x, b/2) = 0; \quad -\alpha_2 \leqslant x \leqslant 0, \tag{10h}$$

$$B(0, y) = 0; \quad y < -l \text{ and } y > l, \tag{10i}$$

$$\bar{B}(0, y) = 0; \quad y < -l \text{ and } y > l, \tag{10j}$$

$$B(0, y) = \bar{B}(0, y); \quad -l < y < l, \tag{10k}$$

$$\partial B/\partial x(0, y) = \partial \bar{B}(0, y)/\partial x; \quad -l < y < l. \tag{10l}$$

In view of the symmetry about the line $y = 0$, we need to consider the solution only in the region $-\alpha_2 \leqslant x \leqslant 1 \cap 0 \leqslant y \leqslant b/2$.

Now the partial differential equations (5)–(8) with the boundary conditions (10) will be solved for V, $\bar{V}$ and B, $\bar{B}$.

METHOD OF SOLUTION

The solution method is similar to the solution method of the MHD flow in a rectangular duct problem.[2] We split the solution into two parts:

$$\begin{pmatrix} V \\ B \end{pmatrix} = \begin{pmatrix} V_0 \\ B_0 \end{pmatrix} + \begin{pmatrix} V_1 \\ B_1 \end{pmatrix}, \qquad \begin{pmatrix} \bar{V} \\ \bar{B} \end{pmatrix} = \begin{pmatrix} \bar{V}_0 \\ \bar{B}_0 \end{pmatrix} + \begin{pmatrix} \bar{V}_1 \\ \bar{B}_1 \end{pmatrix}. \tag{11}$$

The solution with the subscript 0 corresponds to the flow in the ducts in which all the walls are insulated (primary flow). The solution with subscript 1 corresponds to the contribution when the mixed boundary condition on the separating wall is taken into account (secondary flow). Thus we have the following sets of differential equations along with the respective boundary conditions for the two flows:

$$\nabla^2 V_0 + M \partial B_0/\partial x = -1, \tag{12}$$

$$\nabla^2 B_0 + M \partial V_0/\partial x = 0, \tag{13}$$

$$V_0 = 0, \qquad B_0 = 0; \quad x = 0, \quad x = 1, \quad -b/2 \leqslant y \leqslant b/2, \tag{14a}$$

$$V_0 = 0, \qquad B_0 = 0; \quad y = \pm b/2, \quad 0 \leqslant x \leqslant 1, \tag{14b}$$

$$\nabla^2 \bar{V}_0 + M \partial \bar{B}_0/\partial x = k, \tag{15}$$

$$\nabla^2 \bar{B}_0 + M \partial \bar{V}_0/\partial x = 0, \tag{16}$$

$$\bar{V}_0=0, \qquad \bar{B}_0=0; \quad x=0, \quad x=-\alpha_2, \quad -b/2\leqslant y\leqslant b/2, \tag{17a}$$

$$\bar{V}_0=0, \qquad \bar{B}_0=0; \quad y=\pm b/2, \quad -\alpha_2\leqslant x\leqslant 0 \tag{17b}$$

and

$$\nabla^2 V_1+M\partial B_1/\partial x=0, \tag{18}$$

$$\nabla^2 B_1+M\partial V_1/\partial x=0, \tag{19}$$

$$V_1=0, \qquad B_1=0; \quad y=\pm b/2, \quad 0\leqslant x\leqslant 1, \tag{20a}$$

$$V_1=0; \quad x=0, \quad x=1, \ -b/2\leqslant y\leqslant b/2, \tag{20b}$$

$$B_1=0; \quad x=1, \ -b/2\leqslant y\leqslant b/2, \tag{20c}$$

$$\nabla^2 \bar{V}_1+M\partial \bar{B}_1/\partial x=0, \tag{21}$$

$$\nabla^2 \bar{B}_1+M\partial \bar{V}_1/\partial x=0, \tag{22}$$

$$\bar{V}_1=0, \qquad \bar{B}_1=0; \quad y=\pm b/2, \ -\alpha_2\leqslant x\leqslant 0, \tag{23a}$$

$$\bar{V}_1=0; \quad x=-\alpha_2, x=0, \ -b/2\leqslant y\leqslant b/2, \tag{23b}$$

$$\bar{B}_1=0; \quad x=-\alpha_2, \ -b/2\leqslant y\leqslant b/2 \tag{23c}$$

and on the separating wall

$$B_1=\bar{B}_1=0; \quad x=0, y<-l \quad \text{and} \quad y>l, \tag{24a}$$

$$B_1=\bar{B}_1; \quad x=0, \ -l<y<l, \tag{24b}$$

$$\partial\bar{B}_1/\partial x=\partial B_1/\partial x+\partial B_0/\partial x-\partial\bar{B}_0/\partial x; \quad x=0, \ -l<y<l. \tag{24c}$$

The solutions for the primary flow and the secondary flow in the right duct (by taking $a_1=1$) are given as

$$V_0(x, y)=\sum_{m=1,3}^{\infty}\frac{4b^2}{m^3\pi^3}\sin\left(\frac{m\pi}{2}\right)\left(1+\frac{\mathrm{ch}(mx/2)\mathrm{sh}[\rho_m(x-1)]}{\mathrm{sh}\rho_m}\right.$$
$$\left.-\frac{\mathrm{sh}(\rho_m x)\mathrm{ch}[M(x-1)/2]}{\mathrm{sh}\rho_m}\right)\cos\left(\frac{m\pi y}{b}\right) \tag{25}$$

$$B_0(x, y)=\sum_{m=1,3}^{\infty}\frac{4b^2}{m^3\pi^3}\sin\left(\frac{m\pi}{2}\right)\left(-\frac{\mathrm{sh}(Mx/2)\mathrm{sh}[\rho_m(x-1)]}{\mathrm{sh}\rho_m}\right.$$
$$\left.+\frac{\mathrm{sh}(\rho_m x)\mathrm{sh}[M(x-1)/2]}{\mathrm{sh}\rho_m}\right)\cos\left(\frac{m\pi y}{b}\right), \tag{26}$$

$$V_1(x, y)=2\sum_{m=1,3}^{\infty}A_m\frac{\mathrm{sh}[\rho_m(x-1)]}{\mathrm{sh}\rho_m}\mathrm{sh}\left(\frac{M}{2}x\right)\cos\left(\frac{m\pi y}{b}\right), \tag{27}$$

$$B_1(x, y)=-2\sum_{m=1,3}^{\infty}A_m\frac{\mathrm{sh}[\rho_m(x-1)]}{\mathrm{sh}\rho_m}\mathrm{ch}\left(\frac{M}{2}x\right)\cos\left(\frac{m\pi y}{b}\right), \tag{28}$$

where

$$\rho_m = \left(\frac{M^2}{4} + \frac{m^2\pi^2}{b^2}\right)^{1/2},$$

sh(x) and ch(x) are sine and cosine hyperbolic functions respectively and the A_m are the unknown constants.

Similarly, by using the Fourier series expansion method, the solutions to the primary and secondary flows in the left duct are given by

$$\bar{V}_0(x, y) = \sum_{m=1,3}^{\infty} \frac{4b^2k}{m^3\pi^3} \sin\left(\frac{m\pi}{2}\right)\left(-1 + \frac{\text{ch}(Mx/2)\text{sh}[\rho_m(x+\alpha_2)]}{\text{sh}(\rho_m\alpha_2)} - \frac{\text{sh}(\rho_m x)\text{ch}[M(x+\alpha_2)/2]}{\text{sh}(\rho_m\alpha_2)}\right)\cos\left(\frac{m\pi y}{b}\right), \tag{29}$$

$$\bar{B}_0(x, y) = \sum_{m=1,3}^{\infty} \frac{4b^2k}{m^3\pi^3} \sin\left(\frac{m\pi}{2}\right)\left(-\frac{\text{sh}(Mx/2)\text{sh}[\rho_m(x+\alpha_2)]}{\text{sh}(\rho_m\alpha_2)} + \frac{\text{sh}(\rho_m x)\text{sh}[M(x+\alpha_2)/2]}{\text{sh}(\rho_m\alpha_2)}\right)\cos\left(\frac{m\pi y}{b}\right), \tag{30}$$

$$\bar{V}_1(x, y) = -2\sum_{m=1,3}^{\infty} \bar{A}_m \frac{\text{sh}[\rho_m(x+\alpha_2)]}{\text{sh}(\rho_m\alpha_2)} \text{sh}\left(\frac{M}{2}x\right)\cos\left(\frac{m\pi y}{b}\right), \tag{31}$$

$$\bar{B}_1(x, y) = 2\sum_{m=1,3}^{\infty} \bar{A}_m \frac{\text{sh}[\rho_m(x+\alpha_2)]}{\text{sh}(\rho_m\alpha_2)} \text{ch}\left(\frac{M}{2}x\right)\cos\left(\frac{m\pi y}{b}\right), \tag{32}$$

where the $\bar{A}_m$ are the unknown constants.

Substituting for $B_0(x, y)$, $B_1(x, y)$, $\bar{B}_0(x, y)$ and $\bar{B}_1(x, y)$ in the mixed boundary conditions (24), the problem may be reduced to the solutions of the following pair of dual series equations:

$$\sum_{m=1,3}^{\infty} A_m \cos\left(\frac{m\pi y}{b}\right) = 0; \quad l \leqslant y \leqslant b/2, \tag{33}$$

$$\sum_{m=1,3}^{\infty} A_m \cos\left(\frac{m\pi y}{b}\right) = \sum_{m=1,3}^{\infty} \bar{A}_m \cos\left(\frac{m\pi y}{b}\right); \quad 0 \leqslant y \leqslant l, \tag{34}$$

$$\sum_{m=1,3}^{\infty} \bar{A}_m \cos\left(\frac{m\pi y}{b}\right) = 0; \quad l \leqslant y \leqslant b/2, \tag{35}$$

$$\sum_{m=1,3}^{\infty} A_m\rho_m \text{cth}\rho_m \cos\left(\frac{m\pi y}{b}\right) + \sum_{m=1,3}^{\infty} \bar{A}_m\rho_m \text{cth}(\rho_m\alpha_2)\cos\left(\frac{m\pi y}{b}\right) = \sum_{m=1,3}^{\infty} \frac{2b^2}{m^3\pi^3}\sin\left(\frac{m\pi}{2}\right)\left(-\rho_m k\frac{\text{sh}(M\alpha_2/2)}{\text{sh}(\rho_m\alpha_2)} - \rho_m\frac{\text{sh}(M/2)}{\text{sh}\rho_m} + \frac{M}{2}k + \frac{M}{2}\right)\cos\left(\frac{m\pi y}{b}\right); \quad 0 \leqslant y < l, \tag{36}$$

where cth(x) is the cotangent hyperbolic function.

Equation (34) shows that

$$\sum_{m=1,3}^{\infty}(A_m-\bar{A}_m)\cos\left(\frac{m\pi y}{b}\right)=0$$

for $0\leqslant y<l$ and equations (33), (35) also give

$$\sum_{m=1,3}^{\infty}(A_m-\bar{A}_m)\cos\left(\frac{m\pi y}{b}\right)=0$$

for $l\leqslant y\leqslant b/2$. Therefore $A_m=\bar{A}_m$. So the pair of dual series equations (33)–(36) is reduced to (after integrating (36) with respect to y)

$$\sum_{m=1,3}^{\infty}A_m\cos\left(\frac{m\pi y}{b}\right)=0;\quad l\leqslant y\leqslant b/2, \tag{37}$$

$$\sum_{m=1,3}^{\infty}A_m\frac{\rho_m}{m}[\mathrm{cth}\rho_m+\mathrm{cth}(\rho_m\alpha_2)]\sin\left(\frac{m\pi y}{b}\right)=$$

$$\sum_{m=1,3}^{\infty}\frac{2b^2}{m^4\pi^3}\sin\left(\frac{m\pi}{2}\right)\left(-\rho_m k\frac{\mathrm{sh}(M\alpha_2/2)}{\mathrm{sh}(\rho_m\alpha_2)}-\rho_m\frac{\mathrm{sh}(M/2)}{\mathrm{sh}\rho_m}+\frac{M}{2}k+\frac{M}{2}\right)\sin\left(\frac{m\pi y}{b}\right);\quad 0\leqslant y<l. \tag{38}$$

SOLUTION OF DUAL SERIES EQUATIONS

As in Sezgin[2] we take the representation for A_m as

$$A_m=\int_0^l f(t)J_0\left(\frac{m\pi t}{b}\right)\mathrm{d}t, \tag{39}$$

where J_0 is the Bessel function of the first kind and zero order and the function $f(t)$ is to be determined.

The first series equation (37) is automatically satisfied by virtue of the identity[5]

$$\sum_{m=1,3}^{\infty}J_0(mt)\cos(mx)=\frac{H(t-x)}{2(t^2-x^2)^{1/2}};\quad x+t<\pi \tag{40}$$

and with the help of the identity

$$\sum_{m=1,3}^{\infty}J_0(mt)\sin(mx)=\frac{H(x-t)}{2(x^2-t^2)^{1/2}}+\int_0^{\infty}\frac{I_0(st)\mathrm{sh}(sx)}{\mathrm{e}^{\pi s}+1}\mathrm{d}s;\quad x+t<\pi \tag{41}$$

the second series equation (38) is reduced to an Abel's integral equation

$$\int_0^y\frac{f(t)}{(y^2-t^2)^{1/2}}\mathrm{d}t=p(y), \tag{42}$$

where

$$p(y)=\frac{2\pi}{b}\Bigg[\frac{2b^3}{\pi^4}\sum_{m=1,3}^{\infty}\frac{\sin(m\pi/2)}{m^4}\left(\frac{M}{2}-\rho_m\frac{\mathrm{sh}(M/2)}{\mathrm{sh}\rho_m}+\frac{M}{2}k\right.$$
$$\left.-\rho_m k\frac{\mathrm{sh}(M\alpha_2/2)}{\mathrm{sh}(\rho_m\alpha_2)}\right)\sin\left(\frac{m\pi y}{b}\right)-\int_0^l f(t)\sum_{m=1,3}^{\infty}\left(\frac{b}{\pi}\frac{\rho_m}{m}[\mathrm{cth}\rho_m\right.$$
$$\left.+\mathrm{cth}(\rho_m\alpha_2)]-2\right)J_0\left(\frac{m\pi t}{b}\right)\sin\left(\frac{m\pi y}{b}\right)\mathrm{d}t-\int_0^l f(t)\int_0^{\infty}\frac{I_0(\pi ts/b)\mathrm{sh}(\pi ys/b)}{1+\mathrm{e}^{\pi s}}\mathrm{d}s\,\mathrm{d}t\Bigg]. \tag{43}$$

Here I_0, K_0 and I_1, K_1 are modified Bessel functions of the first and second kind of order zero and one respectively and $H(x)$ is the Heaviside function.

The solution of Abel's integral equation (42) is given by

$$f(t)=\frac{2}{\pi}\frac{\mathrm{d}}{\mathrm{d}t}\int_0^t \frac{yp(y)}{(t^2-y^2)^{1/2}}\mathrm{d}y \tag{44}$$

and by substitution of $p(y)$, making use of some well known identities,[5] it is reduced to a Fredholm's integral equation of the second kind for $f(t)$:

$$f(t)+\int_0^l K(x,t)f(x)\mathrm{d}x=g(t);\quad 0\leqslant t<l, \tag{45}$$

where the kernel $K(x, t)$ is

$$K(x,t)=\frac{\pi^2 t}{b^2}\left[\sum_{m=1,3}^{\infty} m\left(\frac{b}{\pi}\frac{\rho_m}{m}[\operatorname{cth}\rho_m+\operatorname{cth}(\rho_m\alpha_2)]-2\right)\right.$$
$$\left.\times J_0\left(\frac{m\pi x}{b}\right)J_0\left(\frac{m\pi t}{b}\right)+2\int_0^\infty \frac{sI_0(\pi sx/b)I_0(\pi st/b)}{1+\mathrm{e}^{\pi s}}\mathrm{d}s\right] \tag{46}$$

and

$$g(t)=\frac{2bt}{\pi^2}\sum_{m=1,3}^{\infty}\frac{\sin(m\pi/2)}{m^3}\left(\frac{M}{2}-\rho_m\frac{\operatorname{sh}(M/2)}{\operatorname{sh}\rho_m}+\frac{M}{2}k-\rho_m k\frac{\operatorname{sh}(M\alpha_2/2)}{\operatorname{sh}(\rho_m\alpha_2)}\right)J_0\left(\frac{m\pi t}{b}\right). \tag{47}$$

The analytical solution of Fredholm's integral equation (45) with the kernel (46) and free term (47) is not obtainable. Because of the infinite series and infinite integrals in the kernel and the free term, numerical difficulties arise, especially for the slowly convergent infinite series for large Hartmann number M. Hence we will look further into these quantities as regards their computability.

For large M $\operatorname{cth}\rho_m\approx 1$ and $\operatorname{cth}(\rho_m\alpha_2)\approx 1$, and so the kernel can be written as

$$K(x,t)=\frac{2\pi^2 t}{b^2}\left\{\sum_{m=1,3}^{\infty}\left[\left(m^2+\frac{M^2}{4}\frac{b^2}{\pi^2}\right)^{1/2}-m\right]J_0\left(\frac{m\pi x}{b}\right)J_0\left(\frac{m\pi t}{b}\right)\right.$$
$$\left.+\int_0^\infty \frac{sI_0(\pi sx/b)I_0(\pi st/b)}{1+\mathrm{e}^{\pi s}}\mathrm{d}s\right\}. \tag{48}$$

With the help of the identity in Sezgin[2] (Appendix I, equation (49)), the kernel (48) takes the form

$$K(x,t)=t\int_0^\infty\left[\left(s^2+\frac{M^2}{4}\right)^{1/2}-s\right]J_0(sx)\,J_0(st)\mathrm{d}s$$
$$+2t\int_{M/2}^\infty\left[\left(s^2-\frac{M^2}{4}\right)^{1/2}-s\right]\frac{I_0(sx)I_0(st)}{1+\mathrm{e}^{bs}}\mathrm{d}s. \tag{49}$$

By taking $t=\rho l$ and $x=tl$, the Fredholm's integral equation (45) may be rewritten as

$$\theta(\rho)+\int_0^1 K_1(t,\rho)\theta(t)\mathrm{d}t=h(\rho);\quad 0\leqslant\rho\leqslant 1, \tag{50}$$

where

$$\theta(\rho)=f(l\rho)/l\rho,\qquad h(\rho)=g(l\rho)/l\rho \tag{51}$$

and

$$K_1(t,\rho)=l^2t\left\{\int_0^\infty\left[\left(s^2+\frac{M^2}{4}\right)^{1/2}-s\right]J_0(stl)J_0(s\rho l)\mathrm{d}s\right.$$
$$\left.+2\int_{M/2}^\infty\left[\left(s^2-\frac{M^2}{4}\right)^{1/2}-s\right]\frac{I_0(s\rho l)I_0(stl)}{1+\mathrm{e}^{bs}}\mathrm{d}s\right\}, \tag{52}$$

$$h(\rho)=\frac{2b}{\pi^2}\sum_{m=1,3}^{\infty}\frac{\sin(m\pi/2)}{m^3}\left(\frac{M}{2}+\frac{M}{2}k-\rho_m\frac{\mathrm{sh}(M/2)}{\mathrm{sh}\rho_m}-\rho_m k\frac{\mathrm{sh}(M\alpha_2/2)}{\mathrm{sh}(\rho_m\alpha_2)}\right)J_0\left(\frac{m\pi l\rho}{b}\right). \tag{53}$$

The first infinite integral in the kernel (53) is transformed to a finite integral by using the identity[6]

$$J_0(\alpha t)\,J_0(\alpha x)=\frac{1}{\pi}\int_0^\pi J_0[\alpha(t^2+x^2-2tx\cos\theta)^{1/2}]\mathrm{d}\theta$$

and equation (54) in Appendix II of Sezgin.[2] Finally the Fredholm's integral equation (50) will be solved with the kernel

$$K_1(t,\rho)=2l^2t\left\{\frac{M^2}{16\pi}\int_0^\pi\left[I_1\left(\frac{M}{4}r\right)K_1\left(\frac{M}{4}r\right)+I_0\left(\frac{M}{4}r\right)K_0\left(\frac{M}{4}r\right)\right]\mathrm{d}\theta\right.$$
$$\left.+\int_{M/2}^\infty\left[\left(s^2-\frac{M^2}{4}\right)^{1/2}-s\right]\frac{I_0(sl\rho)I_0(slt)}{1+\mathrm{e}^{bs}}\mathrm{d}s\right\} \tag{54}$$

and

$$h(\rho)=\left(\frac{M}{2}+\frac{M}{2}k\right)\frac{b\pi}{16}\left(1-2\frac{l^2\rho^2}{b^2}\right)-\frac{2b}{\pi}\sum_{m=1,3}^{\infty}\frac{\sin(m\pi/2)}{m^3}\left(\rho_m\frac{\mathrm{sh}(M/2)}{\mathrm{sh}\rho_m}\right.$$
$$\left.+\rho_m k\frac{\mathrm{sh}(M\alpha_2/2)}{\mathrm{sh}(\rho_m\alpha_2)}\right)J_0\left(\frac{m\pi l\rho}{b}\right), \tag{55}$$

where

$$r=l(\rho^2+t^2-2\rho t\cos\theta)^{1/2} \tag{56}$$

and the free term $h(\rho)$ in (53) is modified by using the identity (Sezgin,[2] Appendix III, equation (60))

$$\sum_{m=1,3}^{\infty}\frac{J_0(mt)\sin(m\pi/2)}{m^3}=\frac{\pi}{32}(\pi^2-2t^2);\quad t<\pi/2,\quad x+t<\pi.$$

Now the analytical formulation of the problem is complete and we are left with the numerical computations to obtain the unknown function $\theta(\rho)$. For this purpose the Fredholm's integral equation is reduced to a system of equations for θ with the help of the Gauss–Legendre quadrature formula. By solving this system of equations for θ, one can find f on making use of (51), which in turn leads to the determination of $V_1(x,y)$, $B_1(x,y)$, $\bar{V}_1(x,y)$ and $\bar{B}_1(x,y)$.

By virtue of equation (39) for A_m, the values of the function f can be substituted back in equations (27), (28), (31) and (32) to give

$$V_1(x,y)=2\mathrm{sh}(Mx/2)u(x,y), \tag{57}$$

$$B_1(x,y)=-2\mathrm{ch}(Mx/2)u(x,y), \tag{58}$$

$$\bar{V}_1(x, y)=2\mathrm{sh}(Mx/2)v(x, y), \tag{59}$$

$$\bar{B}_1(x, y)=2\mathrm{ch}(Mx/2)v(x, y), \tag{60}$$

where

$$u(x, y)=\int_0^l f(t)\sum_{m=1,3}^{\infty}\frac{\mathrm{sh}[\rho_m(x-1)]}{\mathrm{sh}\rho_m}J_0\left(\frac{m\pi t}{b}\right)\cos\left(\frac{m\pi y}{b}\right)\mathrm{d}t, \tag{61}$$

$$v(x, y)=\int_0^l f(t)\sum_{m=1,3}^{\infty}\frac{\mathrm{sh}[\rho_m(x+\alpha_2)]}{\mathrm{sh}(\rho_m\alpha_2)}J_0\left(\frac{m\pi t}{b}\right)\cos\left(\frac{m\pi y}{b}\right)\mathrm{d}t. \tag{62}$$

Since the terms $\mathrm{sh}[\rho_m(x-1)]/\mathrm{sh}\rho_m$ and $\mathrm{sh}[\rho_m(x+\alpha_2)]/\mathrm{sh}(\rho_m\alpha_2)$ can be approximated by $\mathrm{e}^{-\rho_m(2-x)}-\mathrm{e}^{-\rho_m x}$ and $\mathrm{e}^{-\rho_m(2\alpha_2-x')}-\mathrm{e}^{-\rho_m x'}$ $(0\leqslant x'\leqslant\alpha_2)$ respectively for large M, we need the following series:

$$\sum_{m=1,3}^{\infty}\mathrm{e}^{-k\rho_m}J_0\left(\frac{m\pi t}{b}\right)\cos\left(\frac{m\pi y}{b}\right), \quad \text{where } k>0.$$

The equivalence of this series has been obtained by using contour integration (Sezgin,[2] Appendix IV) as

$$\sum_{m=1,3}^{\infty}\mathrm{e}^{-k\rho_m}J_0\left(\frac{m\pi t}{b}\right)\cos\left(\frac{m\pi y}{b}\right)=\frac{b}{2\pi}\int_0^{\infty}\mathrm{e}^{-k(s^2+M^2/4)^{1/2}}J_0(st)\cos(ys)\mathrm{d}s$$
$$-\frac{b}{\pi}\int_{M/2}^{\infty}\sin\left[k\left(s^2-\frac{M^2}{4}\right)^{1/2}\right]\frac{I_0(ts)\mathrm{ch}(ys)}{1+\mathrm{e}^{bs}}\mathrm{d}s. \tag{63}$$

Both of these infinite integrals can be transformed to finite integrals containing modified Bessel functions only (Appendix V and VI of Sezgin[2]) by taking $k=2-x$, $k=x$ for $V_1(x, y)$ and $B_1(x, y)$ and $k=2\alpha_2-x'$, $k=x'$ for $\bar{V}_1(x, y)$ and $\bar{B}_1(x, y)$ back in equations (61), (62) and (57)–(60), where $0\leqslant x'\leqslant\alpha_2$. Now the secondary flows $V_1(x, y)$, $B_1(x, y)$, $\bar{V}_1(x, y)$ and $\bar{B}_1(x, y)$ can be written as

$$V_1(x, y)=\frac{bM}{2\pi^2}\mathrm{sh}\left(\frac{Mx}{2}\right)g(x, y), \tag{64}$$

$$B_1(x, y)=-\frac{bM}{2\pi^2}\mathrm{ch}\left(\frac{Mx}{2}\right)g(x, y), \tag{65}$$

$$\left.\begin{aligned}\bar{V}_1(x, y)&=-\frac{bM}{2\pi^2}\mathrm{sh}\left(\frac{Mx'}{2}\right)h(x', y); &(66)\\ \bar{B}_1(x, y)&=-\frac{bM}{2\pi^2}\mathrm{ch}\left(\frac{Mx'}{2}\right)h(x', y); &(67)\end{aligned}\right\}\quad -\alpha^2\leqslant x\leqslant 0,\quad 0\leqslant x'\leqslant\alpha_2,$$

where

$$g(x, y)=\int_0^l f(t)\int_0^{\pi}\left((2-x)\frac{K_1\{(M/2)[(t\cos\theta+y)^2+(2-x)^2]^{1/2}\}}{[(t\cos\theta+y)^2+(2-x)^2]^{1/2}}\right.$$
$$-x\frac{K_1\{(M/2)[(t\cos\theta+y)^2+x^2]^{1/2}\}}{[(t\cos\theta+y)^2+x^2]^{1/2}}+x\frac{K_1\{(M/2)[(t\cos\theta+b-y)^2+x^2]^{1/2}\}}{[(t\cos\theta+b-y)^2+x^2]^{1/2}}$$
$$\left.-(2-x)\frac{K_1\{(M/2)[(t\cos\theta+b-y)^2+(2-x)^2]^{1/2}\}}{[(t\cos\theta+b-y)^2+(2-x)^2]^{1/2}}\right)\mathrm{d}\theta\,\mathrm{d}t, \tag{68}$$

$$h(x', y) = \int_0^l f(t) \int_0^\pi (2\alpha_2 - x') \frac{K_1\{(M/2)[(t\cos\theta + y)^2 + (2\alpha_2 - x')^2]^{1/2}\}}{[(t\cos\theta + y)^2 + (2\alpha_2 - x')^2]^{1/2}}$$

$$- x' \frac{K_1\{(M/2)[(t\cos\theta + y)^2 + x'^2]^{1/2}\}}{[(t\cos\theta + y)^2 + x'^2]^{1/2}} + x' \frac{K_1\{(M/2)[(t\cos\theta + b - y)^2 + x'^2]^{1/2}\}}{[(t\cos\theta + b - y)^2 + x'^2]^{1/2}}$$

$$+ (2\alpha_2 - x') \frac{K_1\{(M/2)[(t\cos\theta + b - y)^2 + (2\alpha_2 - x')^2]^{1/2}\}}{[(t\cos\theta + b - y)^2 + (2\alpha_2 - x')^2]^{1/2}} \, d\theta \, dt. \tag{69}$$

The term $b - y$ in the third and fourth integrals comes from the approximation of $\mathrm{ch}(ys)/(e^{bs} + 1)$ by $\frac{1}{2}e^{-(b-s)y}$.

By adding $V_0(x, y)$, $B_0(x, y)$ from equations (25), (26) to $V_1(x, y)$, $B_1(x, y)$ obtained above, respectively, one can find the velocity $V(x, y)$ and the induced magnetic field $B(x, y)$ for the right channel. Similarly by adding $\bar{V}_0(x, y)$, $\bar{B}_0(x, y)$ from equations (29), (30) to $\bar{V}_1(x, y)$, $\bar{B}_1(x, y)$ obtained above, respectively, the velocity $\bar{V}(x, y)$ and the induced magnetic field $\bar{B}(x, y)$ in the left channel will be found.

RESULTS AND DISCUSSION

The condition $B(0, y) = \bar{B}(0, y)$, $0 \leq y \leq l$, will imply $B_1(0, y) = \bar{B}_1(0, y)$, $0 \leq y \leq l$, since $B_0 = \bar{B}_0 = 0$ on the $x = 0$ wall. From equations (58), (60) and (61), (62)

$$B_1(0, y) = \bar{B}_1(0, y) = 2 \sum_{m=1,3}^{\infty} \int_0^l f(t) J_0\left(\frac{m\pi t}{b}\right) \cos\left(\frac{m\pi y}{b}\right) dt, \tag{70}$$

which is equal to

$$B_1(0, y) = \bar{B}_1(0, y) = \int_0^l f(t) \frac{H(\pi t/b - \pi y/b)}{[(\pi t^2/b)^2 - (\pi y/b)^2]^{1/2}} \, dt. \tag{71}$$

Therefore

$$B(0, y) = \bar{B}(0, y) = \frac{b}{\pi} \int_y^l \frac{f(t)}{(t^2 - y^2)^{1/2}} \, dt; \quad 0 < y < l. \tag{72}$$

By taking $t = y\,\mathrm{ch}\,\theta$,

$$B(0, y) = \bar{B}(0, y) = \frac{b}{\pi} \int_0^{\mathrm{arcch}(l/y)} f(y\,\mathrm{ch}\,\theta) \, d\theta; \quad 0 \leq y < l. \tag{73}$$

The function f is interpolated at the point $y\,\mathrm{ch}\,\theta$ using Gauss–Legendre abscissae in Lagrange interpolation. For $y = 0$ we have

$$B(0, 0) = \bar{B}(0, 0) = \frac{b}{\pi} \int_0^l \frac{f(t)}{t} \, dt. \tag{74}$$

The magnetic field was computed from equations (73) and (74) on the conducting part of the separating wall. For the integrals 24-point Gauss–Legendre integration was used.

The Fredholm's integral equation (50) was reduced to a system of linear algebraic equations by discretizing the integral using the Gauss–Legendre quadrature formula; 24 points were used in the integration to obtain the desired accuracy. The finite integrals (0 to π) in the kernel and in V_1, B_1, $\bar{V}_1$, B_1 were evaluated with 24-point Gauss–Legendre integration. The infinite series in the free term $h(\rho)$ in (55) was summed till a relative accuracy of 1 in 10^5 was achieved. The infinite integral from $M/2$ to ∞ in the kernel (54) was first transformed to the form (by taking $s=M/2u$)

$$\int_{M/2}^{\infty}\left[\left(s^2-\frac{M^2}{4}\right)^{1/2}-s\right]\frac{I_0(sl\rho)I_0(slt)}{1+e^{bs}}\,ds=\frac{M^2}{4}\int_0^1(1-u^2)^{1/2}\frac{1}{u^3}\frac{I_0(l\rho M/2u)I_0(ltM/2u)}{1+e^{bM/2u}}\,du$$
$$-\frac{M^2}{4}\int_0^1\frac{1}{u^3}\frac{I_0(l\rho M/2u)I_0(ltM/2u)}{1+e^{bM/2u}}\,du.$$

The first integral was extended to $[-1, 1]$ and then Gauss–Chebychev quadrature was used; the second integral was evaluated using Gauss–Legendre integration.

Each channel was divided into 441 mesh points by taking the step size $h=0{\cdot}05(\alpha_2=1, b=1)$. In order to reduce the computational work, use was made of the symmetry about $y=0$. The velocity fields $V(x, y)$, $\bar{V}(x, y)$ and the induced magnetic fields $B(x, y)$, $\bar{B}(x, y)$ were calculated in their corresponding channels. For the entire computations double-precision arithmetic was used to ensure the accuracy of the results. However, the solution of the system of linear algebraic equations was in single precision at the time of the computations. This matrix solver is LEQT2F in the IMSL library, which performs Gaussian elimination with partial pivoting and iterative improvement.

Equal-velocity and equal-magnetic-field lines have been drawn for $10 \leqslant M \leqslant 100$ and for several values of $k(=-(\partial P_2/\partial z)/(\partial P_1/\partial z))$ and l (length of the conducting part of the partition). An increase in M leads to the formation of boundary layers near the non-conducting boundaries as in the one-channel (rectangular duct) problem.[2] However, when $k<1$ the electromagnetic effects are more dominant in channel II. This can be verified by looking at the pattern of velocity contours in Figures 2 and 4. In Figure 2 the lines are visibly affected by the magnetic field in channel II as compared with channel I. In Figure 4 the pressure gradient in channel II is insufficient to suppress the effects of the magnetic field in channel II, but the pattern is maintained somewhat in channel I

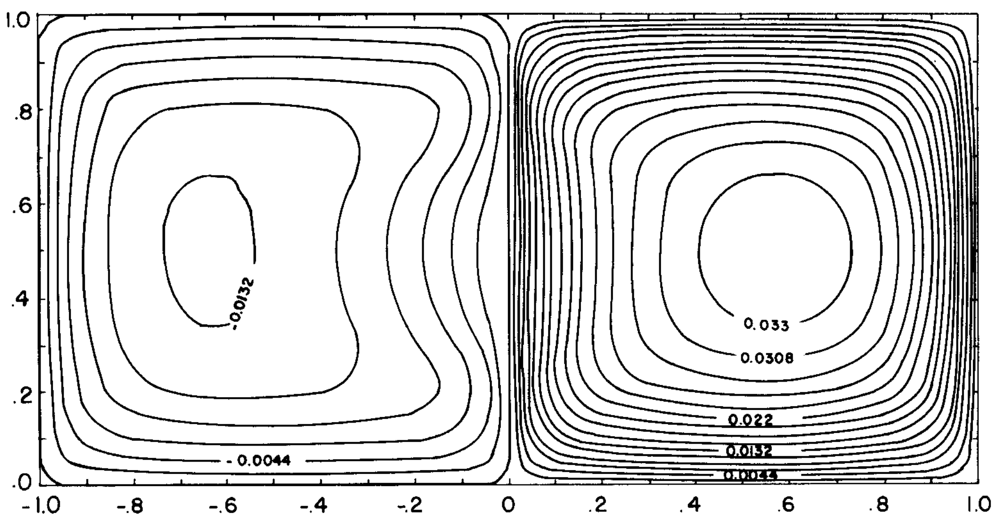

Figure 2. Velocity lines for $M=10$, $k=0{\cdot}5$, $l=0{\cdot}25$

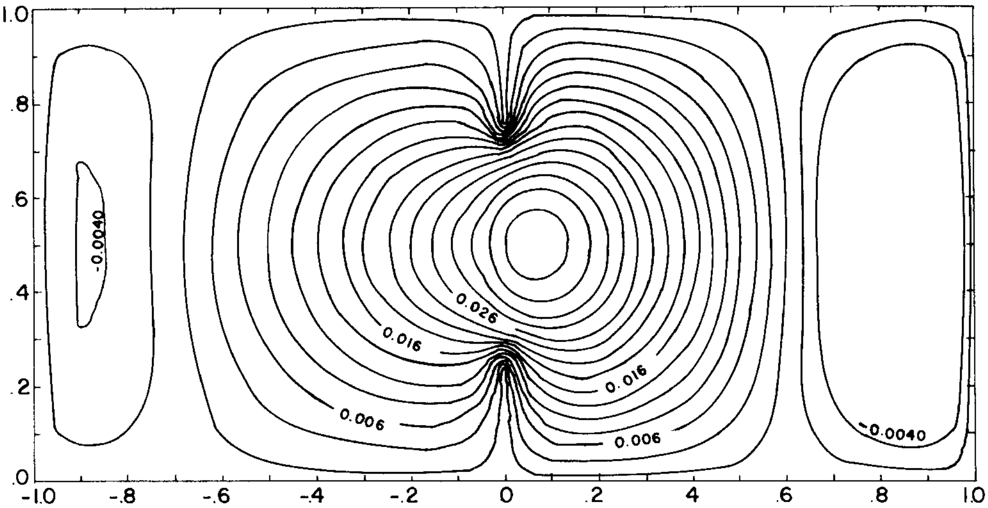

Figure 3. Magnetic field lines for $M = 10$, $k = 0{\cdot}5$, $l = 0{\cdot}25$

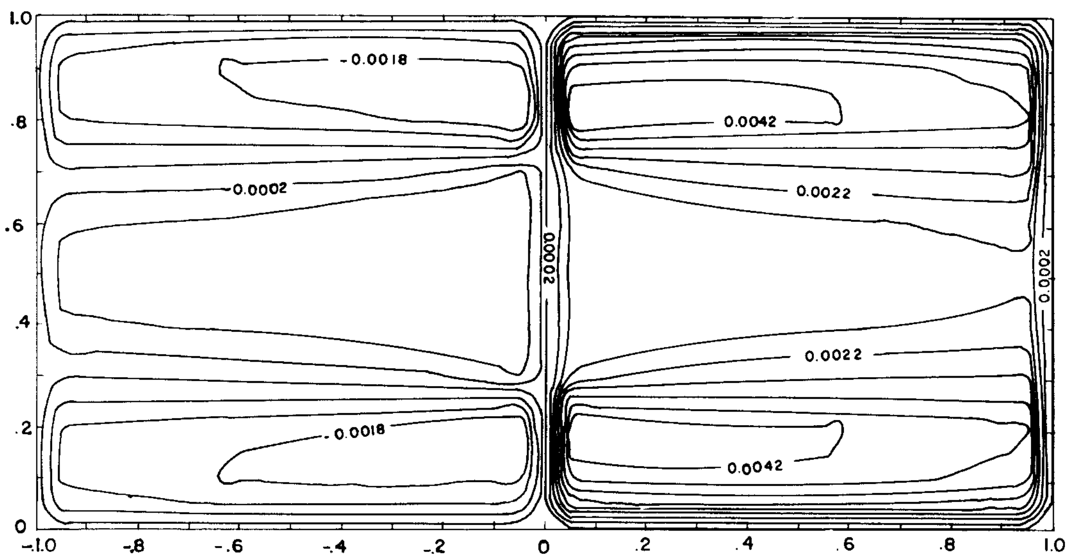

Figure 4. Velocity lines for $M = 100$, $k = 0{\cdot}5$, $l = 0{\cdot}25$

because of a larger value of the pressure gradient. For larger values of M electromagnetic effects predominate over the effects of pressure gradient in both channels, as can be seen in Figures 4 and 10 for $M = 100$ and $M = 50$ respectively. Also we note that an increase in M gives rise to reversal of the flow direction in channel II in the region adjoining the conducting part. This result is similar to that derived by Butsenieks and Shcherbinin.[3]

The effect of varying M on current lines (equal-magnetic-field lines) has been depicted in Figures 3, 5 and 11. The current induced in channel I is partially closed (negative lines), and the

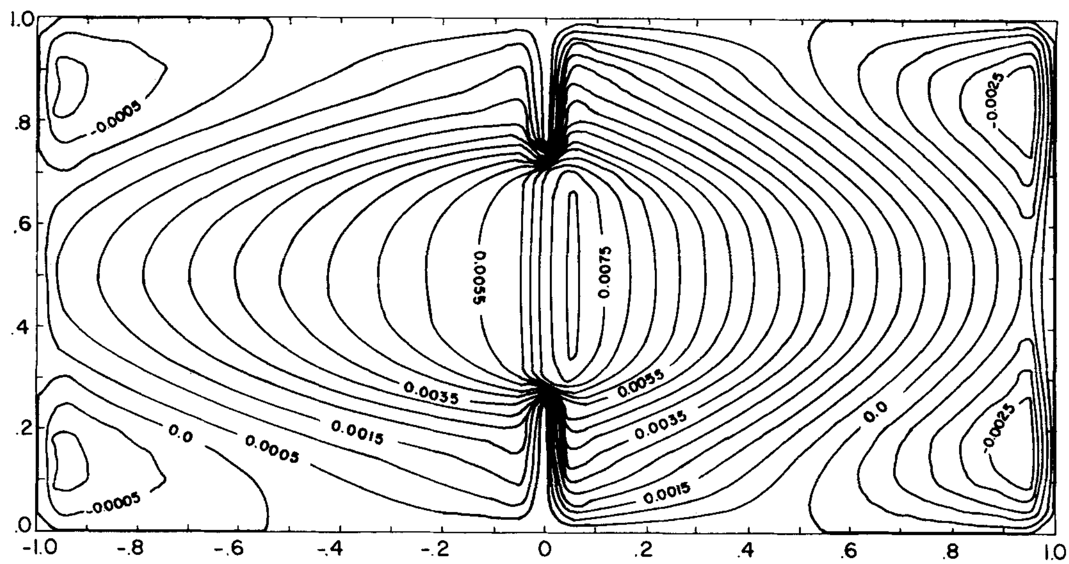

Figure 5. Magnetic field lines for $M=100$, $k=0{\cdot}5$, $l=0{\cdot}25$

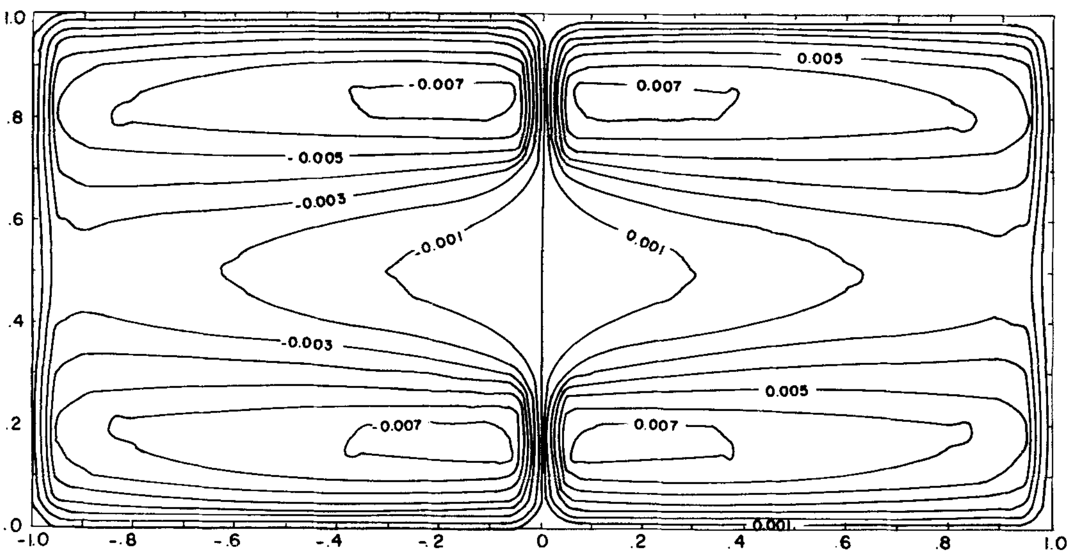

Figure 6. Velocity lines for $M=50$, $k=1$, $l=0{\cdot}25$

rest of the current is connected to the fluid in channel II through the conducting partition. Also the pattern of current lines is similar to that for a rectangular duct.[2]

Next we consider various values of k for $M=50$ and $l=0{\cdot}25$ in Figures 6–8. For $k=1$ the negative velocities in channel II are equal in magnitude to the positive velocities in channel I (Figure 6). We note that when the counter pressure in the second channel (k) is reduced by a ratio

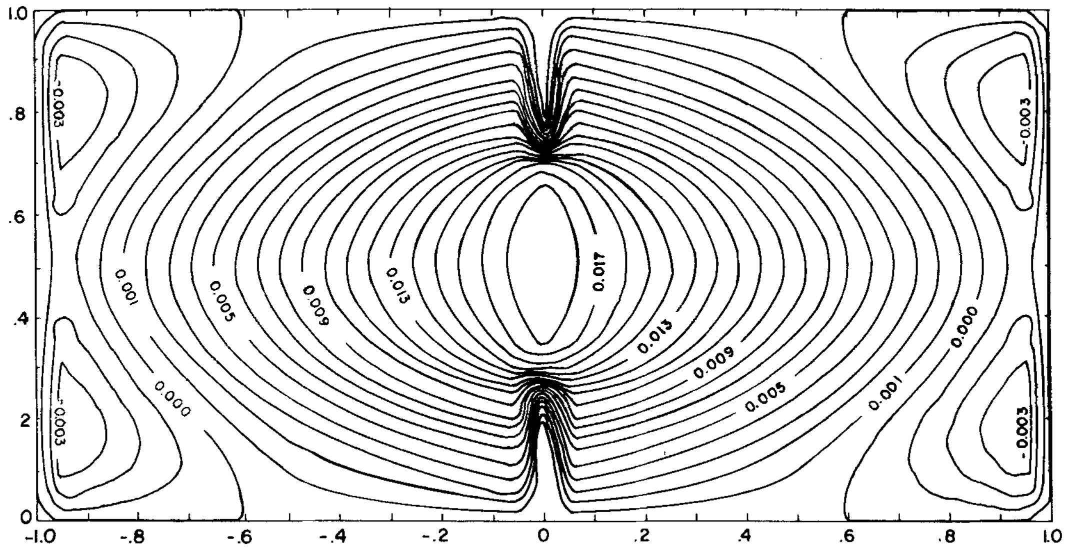

Figure 7. Magnetic field lines for $M=50$, $k=1$, $l=0{\cdot}25$

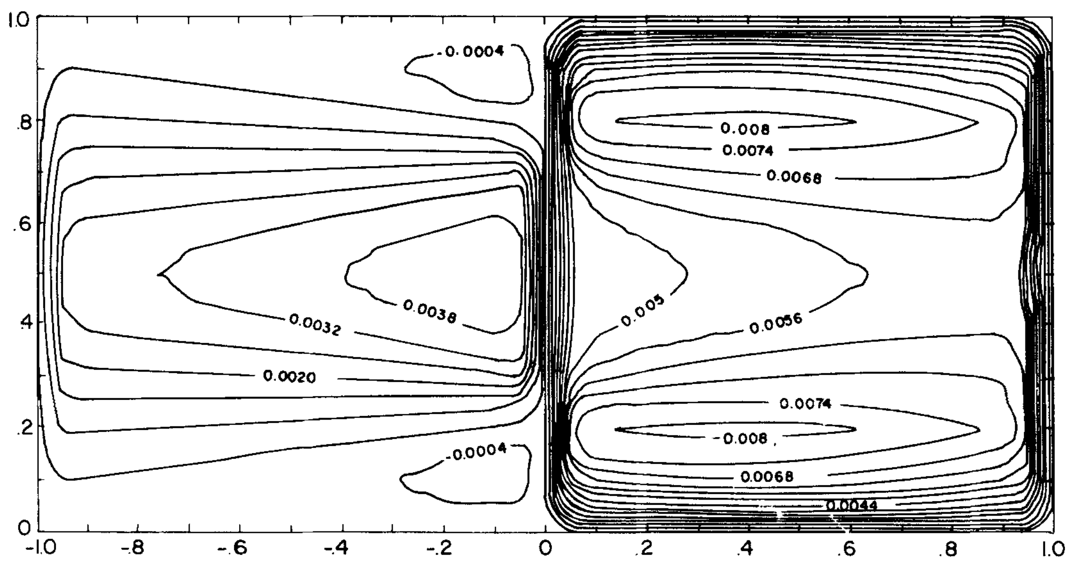

Figure 8. Velocity lines for $M=50$, $k=0{\cdot}1$, $l=0{\cdot}25$

of 1 : 10, there is almost complete reversal of the flow in channel II (Figures 6 and 8), the flow in channel I being affected only marginally. But in channel II the flow in the opposite direction is confined to a very narrow region near the non-conducting part of the partition. It is also noted that in channel II the velocity is lower than in the core.

A similar contrast can be seen from Figures 7 and 9 in the pattern of current lines when k is varied. It may be noted from Figure 7 that there is no region in channel II in which the current

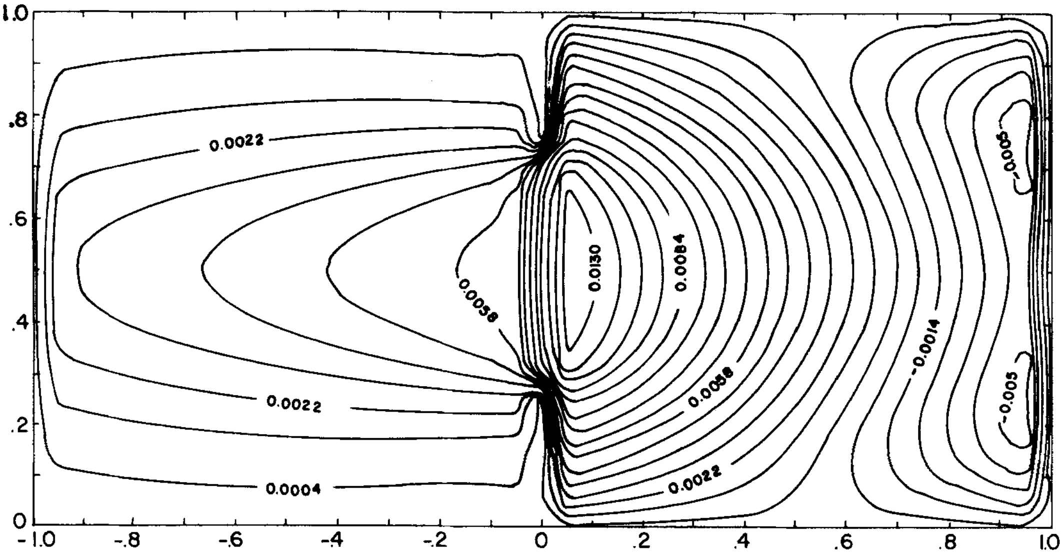

Figure 9. Magnetic field lines for $M=50$, $k=0{\cdot}1$, $l=0{\cdot}25$

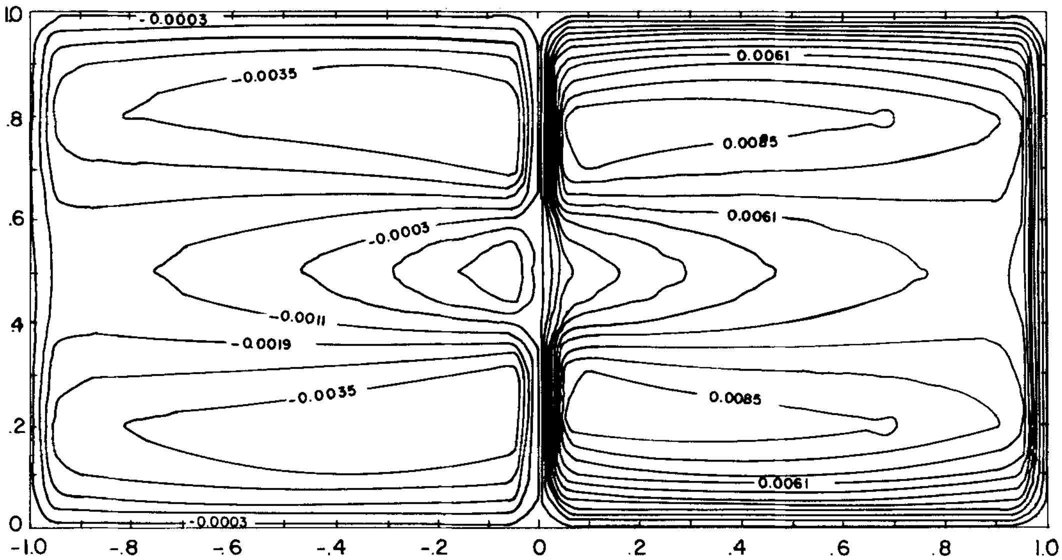

Figure 10. Velocity lines for $M=50$, $k=0{\cdot}5$, $l=0{\cdot}15$

lines characterized by negative values of B seem to exist. It may also be noted that a similar conclusion was arrived at by Butsenieks and Shcherbinin.[3] We further notice that the point where maximum B occurs tends to move in the first channel as the ratio of the pressure gradients is varied.

The comparison of equal-velocity lines and current lines for several values of l but for given $M=50$, $k=0{\cdot}5$ is presented in Figures 10–13, which are equal-velocity lines for $l=0{\cdot}15$ and

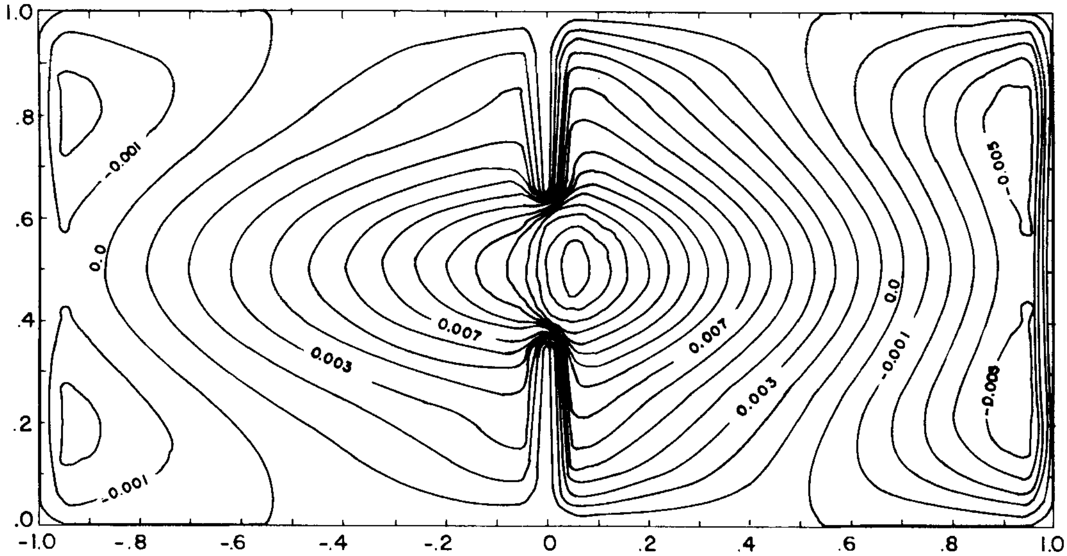

Figure 11. Magnetic field lines for $M=50$, $k=0{\cdot}5$, $l=0{\cdot}15$

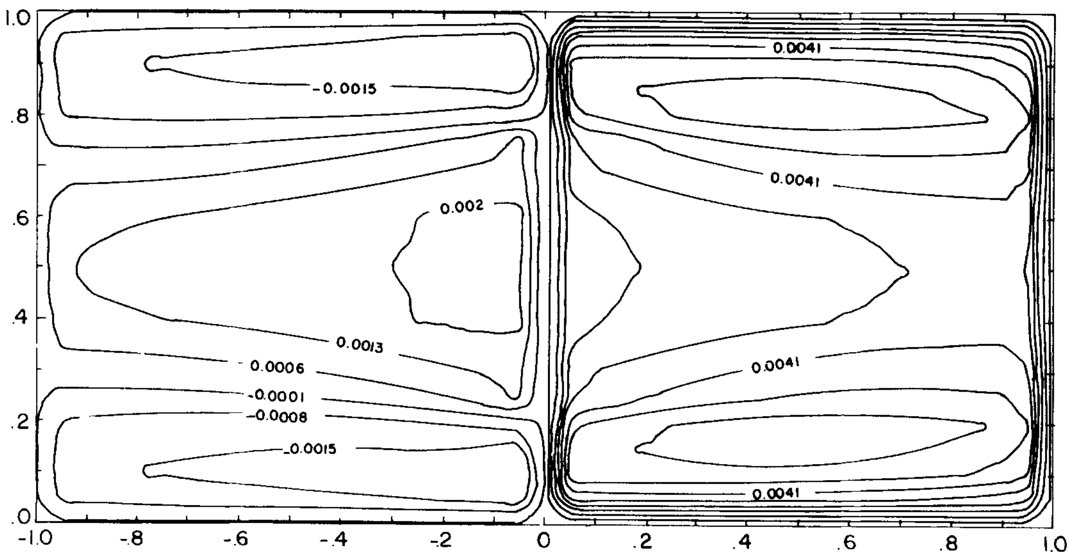

Figure 12. Velocity lines for $M=50$, $k=0{\cdot}5$, $l=0{\cdot}35$

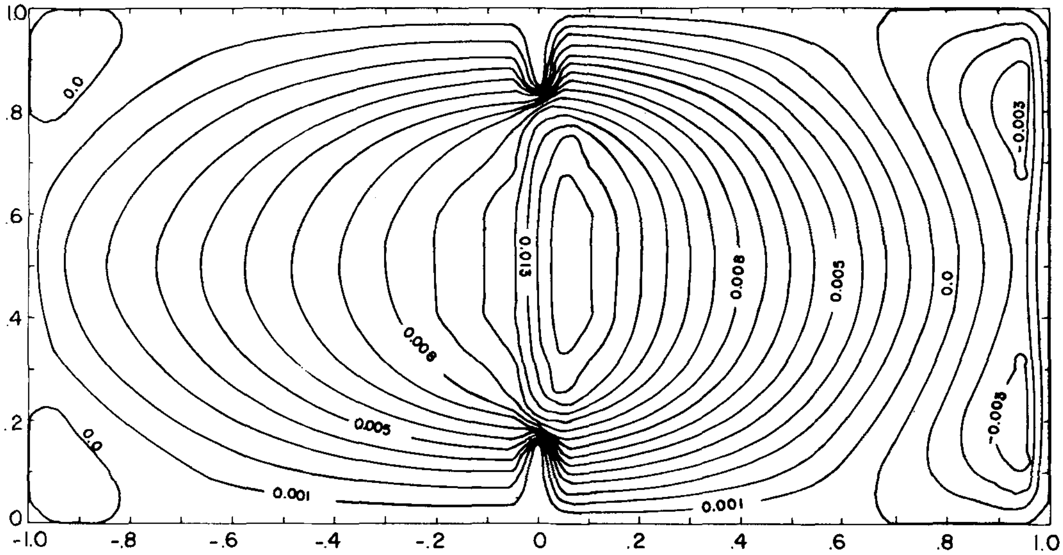

Figure 13. Magnetic field lines for $M=50$, $k=0{\cdot}5$, $l=0{\cdot}35$

0·35 respectively. The pattern of velocity and current lines with varying l is similar to that for a rectangular duct.[2]

The behaviours of the equal-velocity lines and the current lines are in very good agreement with Butsenieks and Shcherbinin's[3] results, which are obtained for the special case $l=b/2$ in their paper (partition was conducting).

Table I

Hartmann number M	l	k	Q_1	Q_2
50	0·25	0·90	0·0041	−0·00330
50	0·25	0·80	0·0043	−0·00270
50	0·25	0·50	0·0049	−0·00094
50	0·25	0·35	0·0052	−0·00005
50	0·25	0·30	0·0053	−0·00025
50	0·25	0·10	0·0057	−0·00143
50	0·15	0·50	0·0062	−0·00220
50	0·25	0·50	0·0049	−0·00094
50	0·35	0·50	0·0039	0·00011
10	0·25	0·50	0·0203	−0·00800
20	0·25	0·50	0·0115	−0·00340
50	0·25	0·50	0·0049	−0·00094
100	0·25	0·50	0·0026	0·00110

In Table I we present the integrated flow rates in both channels calculated from the equations

$$Q_1=\int_{-b/2}^{b/2}\int_0^1 V(x,y)\mathrm{d}x\mathrm{d}y=\int_{-b/2}^{b/2}\int_0^1 [V_0(x,y)+V_1(x,y)]\mathrm{d}x\mathrm{d}y$$

$$=-\sum_{m=1,3}^{\infty}\frac{16b^3}{m^4\pi^4}\sin^2\left(\frac{m\pi}{2}\right)\frac{\rho_m}{M^2/2-\rho_m^2}\left(\frac{\mathrm{e}^{-\rho_m}(\mathrm{e}^{M/2}+\mathrm{e}^{-M/2})-1-\mathrm{e}^{-2\rho_m}}{1-\mathrm{e}^{-2\rho_m}}-\frac{M^2/4-\rho_m^2}{2\rho_m}\right)$$

$$+\int_0^l f(t)\sum_{m=1,3}^{\infty}\frac{2b}{m\pi}\sin\left(\frac{m\pi}{2}\right)J_0\left(\frac{m\pi t}{b}\right)\left(\frac{M}{M^2/4-\rho_m^2}-\frac{2\rho_m}{M^2/4-\rho_m^2}\frac{\mathrm{e}^{-\rho_m}(\mathrm{e}^{M/2}-\mathrm{e}^{-M/2})}{1-\mathrm{e}^{-2\rho_m}}\right)\mathrm{d}t,$$

$$Q_2=\int_{-b/2}^{b/2}\int_{-\alpha_2}^{0}\bar{V}(x,y)\mathrm{d}x\mathrm{d}y=\int_{-b/2}^{b/2}\int_0^1 [-kV_0(x,y)-V_1(x,y)]\mathrm{d}x\mathrm{d}y$$

$$=\sum_{m=1,3}^{\infty}\frac{16b^3k}{m^4\pi^4}\sin^2\left(\frac{m\pi}{2}\right)\frac{\rho_m}{M^2/4-\rho_m^2}\left(\frac{\mathrm{e}^{-\rho_m}(\mathrm{e}^{M/2}+\mathrm{e}^{-M/2})-1-\mathrm{e}^{-2\rho_m}}{1-\mathrm{e}^{-2\rho_m}}-\frac{M^2/4-\rho_m^2}{2\rho_m}\right)$$

$$-\int_0^l f(t)\sum_{m=1,3}^{\infty}\frac{2b}{m\pi}\sin\left(\frac{m\pi}{2}\right)J_0\left(\frac{m\pi t}{b}\right)\left(\frac{M}{M^2/4-\rho_m^2}-\frac{2\rho_m}{M^24-\rho_m^2}\frac{\mathrm{e}^{-\rho_m}(\mathrm{e}^{M/2}-\mathrm{e}^{-M/2})}{1-\mathrm{e}^{-2\rho_m}}\right)\mathrm{d}t$$

for $\alpha_2=1$, which are obtained from equations (25), (27).

The integrated flow rate Q_2 in channel II becomes zero for some k in $0{\cdot}3<k<0{\cdot}35$.

ACKNOWLEDGEMENT

This work was supported by the Scientific and Technical Research Council of Turkey.

REFERENCES

1. M. Sezgin, 'Magnetohydrodynamic flow in an infinite channel', *Int. j. numer. methods fluids*, **6**, 593–609 (1986).
2. M. Sezgin, 'Magnetohydrodynamic flow in a rectangular duct', *Int. j. numer. methods fluids*, **7**, 697–718 (1987).
3. I. E. Butsenieks and E. V. Shcherbinin, 'Magnetohydrodynamic flow in electrodynamically coupled rectangular ducts, I', *Magn. Girodinam.*, **2,** 35–40 (1976).
4. L. Dragos, *Magnetofluid Dynamics*, Abacus Press, 1975.
5. I. S. Gradshteyn and I. M. Ryzhik, *Tables of Integrals, Series and Products*, Academic Press, New York and London, 1965.
6. G. Eason, B. Noble and I. N. Sneddon, 'On certain integrals of Lipschitz–Hankel type involving products of Bessel functions', *Phil. Trans. Roy. Soc., Series A*, **247,** 529–551 (1955).